Aug. 30, 2010

Dr. Philippe Crane
Solar System Division
Office of Space Science
NASA Headquarters
Washington, DC 20546-0001

Dear Dr. Crane,

You will find enclosed my final report for grant NNG06-GG20G titled "Non-thermal Production of Atomic and Molecular Oxygen and Hydrogen in Saturn's Ring Atmosphere." We examined the formation of hydrogen and oxygen from ices and also focused on the role of the particle interface on the formation and release of oxygen. There was a no-cost extension of this project so we also worked extensively on the issue of electron-beam induced population of the Mercury's exosphere via stimulated desorption from simulated regolith material. I attach the abstracts of recent papers on this topic. Please let me know if any additional information is required.

Sincerely,

Thomas M. Orlando
Professor
School of Chemistry and Biochemistry
Georgia Institute of Technology
(404) 894-4012
FAX (404) 894-7452
Thomas.Orlando@chemistry.gatech.edu

Final Report
NASA Planetary Atmospheres Program
"Non-thermal Production of Oxygen and Hydrogen in Saturn's Ring Atmosphere"
NNG06-GG20G
For the period May 1, 2006 – Jan. 31, 2010
Thomas M. Orlando, Principal Investigator

A. Summary of Progress

During grant NNG-06GG0G5, we examined the stimulated formation and thermally induced release of molecular hydrogen and oxygen from porous nano-scale ice samples. We also examined the water graphite interface and probed the stimulated reactions and energy transfer at the graphite water ice interface. Specifically, we have shown that the formation and release of H_2 and O_2 from pristine ice are associated with the presence of intrinsic pores. In fact, the production of H_2 and O_2 occurs primarily at interfaces and grain boundaries and the release of H_2 occurs primarily when the pores collapse whereas O_2 is retained until ice undergoes an amorphous to cubic-phase transition. We have found (i) a correlation between quiescent retention of radiolytic generated gases and the migration of electronic excitations through ice, (ii) made continued progress in modeling the kinetics of ice radiolysis and radiation induced defect-mediated processing of ice, and (iii) applied this model to understanding near-threshold vacuum ultraviolet photon induced production of H_2 and O_2. The work with graphite indicates that the water interface structure is very different than water on metals or metal oxides. There is a propensity for hydrogen interactions and a clear indication of reactive scattering of atomic oxygen and hydrogen. The former can lead to the production of CO and CO_2 whereas the latter likely contributes to HCO formation. In the presence of nitrogen, HCNO or HOCN formation also occurs.

During the no-cost extension phase of grant NNG06-GG20G, we examined the potential role of electron-stimulated desorption (ESD) in the formation of Mercury's exosphere. Experimental results involving electron irradiation of Na- and K-bearing silicate glasses yielded direct desorption of H^+, H_2^+, O^+, H_3O^+, Na^+, K^+ and O_2^+. The estimated total cross-section for ESD at a surface temperature of 400 K is $\geq 10^{-19}$ cm^2; much larger than neutral production followed by electron impact ionization or photoionization in the gas-phase. These results indicate that ESD may contribute significantly to the production and release of regolith constituents, particularly in ionic form, directly into the exosphere of Mercury.

PROJECT 1. Effect of pores and interfaces on stimulated production and release of gaseous molecules.

This trapping and release of H_2 and O_2 occurs, especially during irradiation and heating of porous amorphous ice. We have examined this further by carrying out quantum state-resolved measurements of atomic hydrogen and oxygen release during the heating of ice. These atomic fragments were detected using resonance enhanced multiphoton ionization (REMPI) of the O (^3P_J) and H (^2S) using the frequency tripled output of the Nd:YAG pump dye laser. An interesting enhanced release in the hydrogen atom signal was observed during the collapse of pores. This can be seen in Figure 1 below.

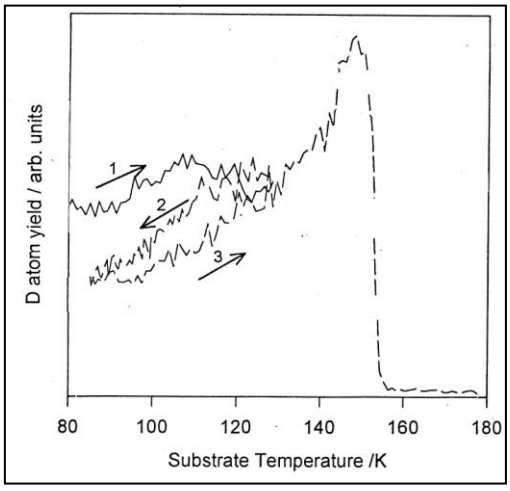

Figure 1. Production and release of atomic hydrogen as a function of ice temperature. The enhanced signal as you proceed from 1 to 2 is related to the collapse of micro-pores. The increased signal at 150K is related to the formation of crystalline ice and the drop above 155K is due to sublimation.

This enhanced release from 90-120 K is not observed in the atomic or molecular oxygen signals. However, Figure 2 shows that molecular oxygen may be trapped and released. To understand this, we carried out formation and release experiments as a function of ice phase, electron dose and temperature.

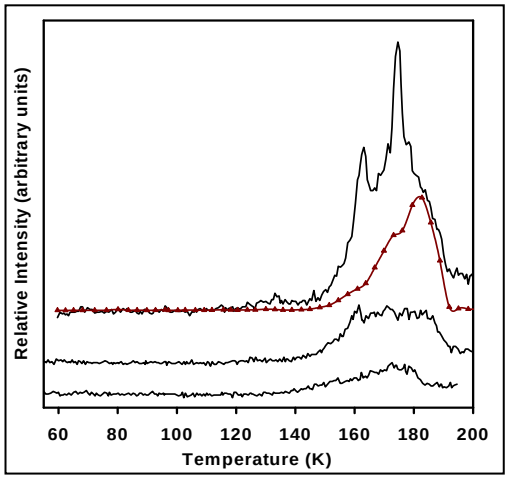

Figure 2. Release of trapped molecular oxygen which has been formed by electron-irradiation as a function ice phase (bottom – crystalline ice, middle is amorphous ice and top is highly porous ice dosed at 50K and 50^o incident angle. The red trace is pure water temperature programmed desorption). Note the oxygen is released primarily during the amorphous to cubic phase transition.

PROJECT 2. Electron-stimulated reactions on water covered graphite surfaces.

An important element of this program is to examine the role of the substrate and interfacial energy or charge exchange on the stimulated production and release of oxygen and hydrogen. The electronic structure of the substrate interface and coupling to adsorbed water affects the radiolytic decomposition channels that result in hydrogen and oxygen production. We have also found that an oxidizable substrate such as graphite can interfere with the sequential process of generating oxygen precursors and consume them, while simultaneously generating CO, CO_2 and other oxygen functionalized organic molecules.

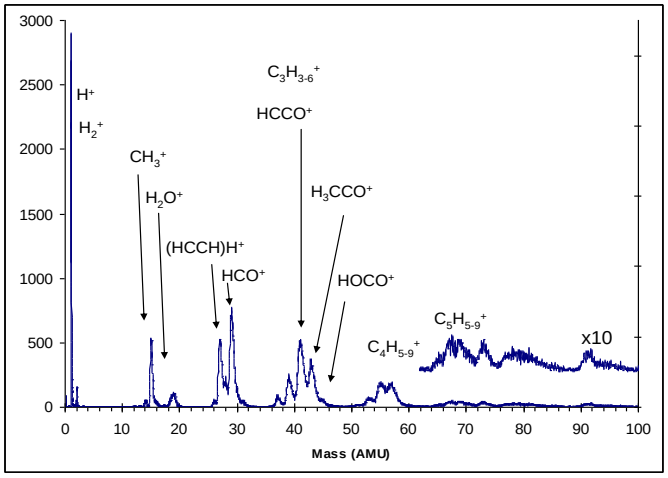

Figure 3. Time of flight mass spectra of ions produced and desorbed from electron irradiation of graphite surfaces containing trace amounts of water and oxygen. Note the formation of higher mass hydrocarbons and the formation of oxygen containing products.

Figure 3 shows the rich spectra of products desorbed from a clean graphite surface which contains trace amounts of water and nitrogen. The substrate temperature was 45 K. Electron irradiation ejects carbon-containing ionic fragments into the gas phase, however, there are also higher mass hydrocarbons and oxygen containing products which clearly arise from the substrate and reactive scattering events.

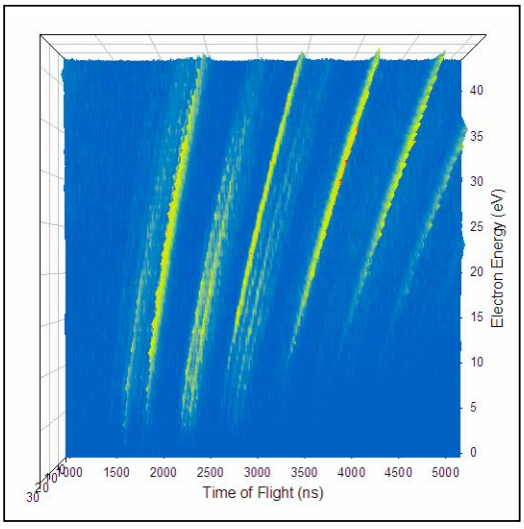

Figure 4. Flight time distributions (X axis) versus incident electron energy (Y axis). Spectrum shows organic and protonated water cluster ions desorbed from graphite surface. Flight times shift to longer values when higher energy electrons induce surface charge which retards the escape of the cations.

As shown in figure 4, stimulated reactions at the graphite interface can also be used to probe charging. Incident low energy electron radiation can become trapped in the interface, resulting in net charge accumulation. The energy of the outgoing ions is influenced by Coulombic attraction or repulsion, resulting in shifts of their flight time. We have observed this effect on the organic and water-group ion emission from graphite. Under these conditions the oxygen from water is being consumed by the formation of oxidized carbon compounds, reducing the amount available for O and O_2 generation.

PROJECT 3. Reactive scattering of oxidants with ice inclusions.

Since ices in nature rarely occur in pristine form, studies of the effect of trace amounts of co-adsorbed species and inclusions of dust grains are needed to fully compare laboratory measurements to real systems. We have found that the presence of small organic molecules significantly affects the reaction sequence that normally results in O_2 generation. Significantly, we have seen that adsorption of methane, dosed into ice pores, will create CO_2 from H_2O radiolysis induced oxidation, and simultaneously encapsulate it into pockets. Co adsorption studies of CO_2 with ice always exhibit a low temperature (70 K) feature due to surface desorption. Our post-irradiation thermal desorption studies (shown in Figure 5) show clearly that the low temperature feature is absent, CO_2 almost exclusively escapes during the amorphous to cubic phase transition, indicating that all of the CO_2 is trapped within pores.

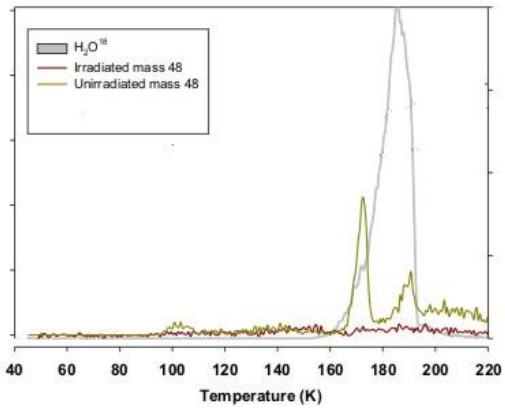

Figure 5. Post-irradiation thermal desorption spectrum of O^{18} isotope labeled CO_2 generated from irradiation of organically doped ice.

PROJECT 4: The potential role of electron-stimulated desorption (ESD) in the formation of Mercury's exosphere.

A simulation has carried out by members of the MERCURY mission team indicate regions of Mercury's surface can be bombarded with electron fluxes ~10^{10} $cm^{-2}s^{-1}$ with average energies up to 500 eV. As shown in Figure 6, our experimental results involving electron irradiation of Na- and K-bearing silicate glasses yielded direct desorption of H^+, H_2^+, O^+, H_3O^+, Na^+, K^+ and O_2^+. Threshold energies for production/release of ions have been measured to be 25±2 eV for H^+, 30±2 eV for O^+, Na^+ and K^+, 40±2 eV for H_2^+ and H_3O^+, and 90±2 eV for O_2^+. The 25-30 eV thresholds correlate with deep valence holes in the O 2s levels that undergo Auger decay. The thresholds for H_2^+ and H_3O^+ correspond to two-hole states in chemisorbed water, which produce energetic protons that undergo reactive scattering on the surface. A significant increase in ESD yield of all ions is observed above a substrate temperature of 350 K. The estimated total cross-section for ESD at a surface temperature of 400 K is $\geq 10^{-19}$ cm^2; much larger than neutral production followed by electron impact ionization or photoionization in the gas-phase. These results indicate that ESD may contribute significantly to the production and release of regolith constituents, particularly in ionic form, directly into the exosphere of Mercury.

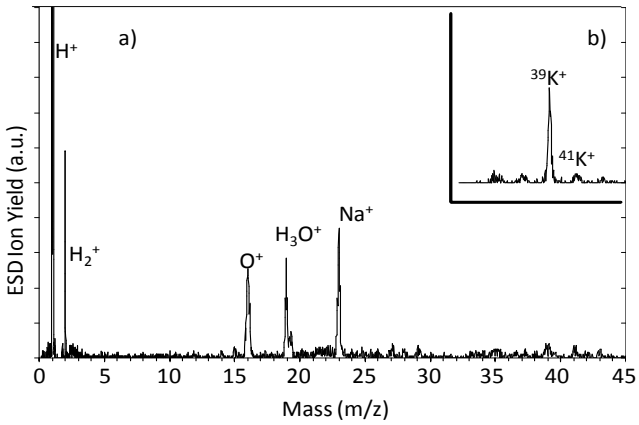

Figure 6. (a) Electron stmulated desorption time-of-flight (ToF)mass spectrum from a glassy silicate containing Na. Typically, the H^+ ion yield is 50 times that of H_2^+, O^+, H_3O^+, Na^+. (b) Inset is the ESD ToF spectrum obtained from the K containing silicate glass with only the two major isotopes of K^+ shown.

3.1. Mechanisms of Electron Stimulated Desorption of Ions from Silicates

It is well known that ESD of ions from wide band-gap materials involves ionization of deep valence, shallow core, and/or deep core levels followed by a complicated multi-electron Auger relaxation process. This is often referred to as the

Knotek-Fiebelman (KF) or Auger stimulated desorption process and is useful in qualitatively explaining the general production and removal of ions from maximum valence materials such as metal oxides Figures 7 is a schematic depiction of the interatomic potentials and deep valence, shallow core and deep core levels of the atomic components of the Na-bearing silicate glasses. The KF mechanism is depicted by the sequence of arrows and involves hole production in either deep valence, shallow core and/or deep core holes, Auger decay, reversal of the Madelung potential, and ion expulsion due to the resultant Coulomb repulsion. While O is nominally a 2^- oxidation state, in real minerals and in radiation damaged crystals, defects exists that contain O^-. On Mercury's surface, because of the intense solar irradiation, defects could be abundant. The oxidation state of O located at a defect site can have a partial charge closer to O^- that can balanced by H or non-structural cations. The thresholds for Na^+ and K^+ removal at 30 eV can therefore be attributed to ionization of the O 2s level. This hole is filled via Auger decay using charge density in the O 2p level. Since energy is gained in the Auger decay, an electron is emitted leaving behind an O^+ ion. This reversal of the Madelung potential leaves the Na^+/K^+ in the vicinity of an O^+ and Si^{4+} site. The primary O^+ thresholds near 30 eV can also be attributed to excitation/ionization of the O 2s level in SiO_2.

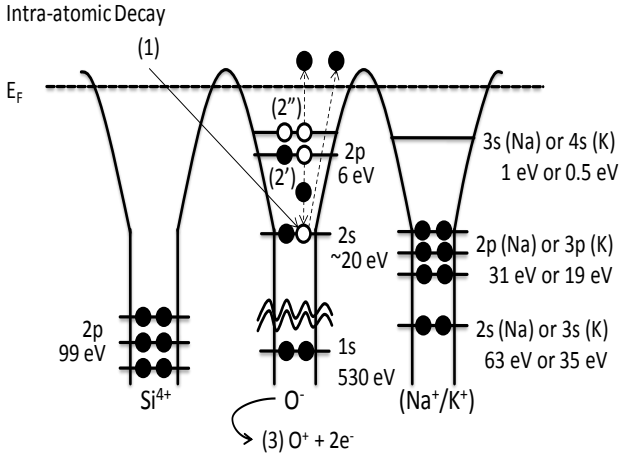

Figure 7. Auger stimulated desorption model for desorption of O^+, Na^+, K^+ and Si^+ ions, (*n.b.*, energies not drawn to scale). 1) The incident electron can create a hole on the non-bridging O in the 2s level. Note, the incident electron scatters and its final state is not shown above. 2') The system can undergo intra-atomic Auger decay using charge density in the O 2p level. 2") Depicts the simultaneous ejection of an additional O 2p electron, which leads to 3) O^+ or Na^+/K^+ ejection via Coulomb repulsion between the resultant O^+, Na^+/K^+ and the Si^{4+} sites.

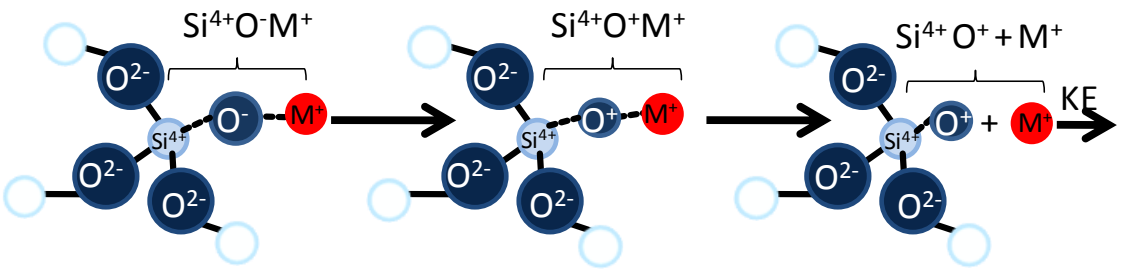

Figure 8. A schematic representation of the stimulated desorption of alkali metal ions (M^+ = Na^+ or K^+) bonded to an oxygen defect site on the surface of the silicate matrix. Note, M^+ could also possibly be H^+. The desorption for the alkali metals occur via intra- and interatomic Auger decay processes yielding a desorbing ion with a kinetic energy (KE) of 3-10 eV.

The H_2^+ and H_3O^+ have higher ESD threshold energies (~ 40 eV) that likely correspond to two-hole states in surface hydroxyls or chemisorbed water, which produce energetic protons that can reactively scatter. We conclude that the H_2^+ is indeed due to reactive scattering of an energetic proton with an adjacent water molecule or surface hydroxyl. We also conclude that the formation and release of H_3O^+ can involve a similar reactive scattering process. The higher threshold energy also indicates the likely role of a two-hole state localized on a water dimer or surface hydroxyl water complex.

It is important to note that the Coulomb explosion resulting from Auger cascading events typically ejects the ions with kinetic energies between 3 - 10 eV. This is the energy necessary to prevent any recapture by the surface and may enable the direct ejection of ions from Mercury into the exosphere. This pertains to all of the ions observed in our ESD study. Thus, ESD could be one of the source terms for the O^+, Na^+ and K^+ originally observed in the near surface region during the first and second flybys. While the plethora of ions found in close Mercury proximity by FIPS is not surprising in hindsight, this is an important discovery and changes the general way that planetary scientists perceive Mercury's space environment.

Publications and Presentations:

T. M. Orlando, "The formation of reactive atomic fragments via dissociative recombination, dissociative electron attachment and Coulomb explosions", European Group on Atomic and Molecular Physics, Ischia, Italy May, 2006.

G.A. Grieves, T.M. Orlando and R.E. Johnson "Surface desorption of molecular oxygen and hydrogen by VUV photon and electron stimulated desorption of ices relevant to Saturn's rings." Poster presented at 2006 Fall AGU Meeting, December 11, 2006.

G.A. Grieves, T.M. Orlando, A. Alexandrov and C. Paty, "Degradation and hydrogen and oxygen release via electron bombardment of icy Jovian satellite surfaces." Poster presented at 2006 Fall AGU Meeting, December 11, 2006.

Orlando, T.M., Grieves, G.A. "The formation and fate of oxidants on icy satellite surfaces." Fall AGU December 2007.

Orlando, T.M., Grieves, G.A., Alexandrov, A., McCord, T. "The perturbation of near IR optical features of water ice induced by frozen acids, brines and organic polymers." Fall AGU December 2007.

G. A. Grieves and T. M. Orlando, Contributed Talk: "Low energy electron-induced desorption as a potential source for exosphere formation", American Geophysical Society Meeting, Dec.14-18, 2009.

D. Dyar, C. A. Hibbits amd T. M. Orlando, "Mechanisms for incorporation of hydrogen in and on terrestrial planetary surfaces", Lunar Planet. Sci. 41, abstract 2116 (2010).

Hibbitts C. A. * Dyar M. D. Orlando T. M. Grieves G. Moriaty D. Poston M. Johnson A. "Thermal stability of water and hydroxyl on airless bodies"., Lunar Planet. Sci. 41, abstract 2417 (2010).

T. B. McCord, L. A. Taylor, T. M. Orlando, C. M. Pieters, Combe J.-Ph., Kramer, G., Sunshine, J. M. , Head, J. W. Mustrad, J. F. et al., "Origin of OH/Water on the lunar surface detected by the moon mineralogy mapper", Lunar Planet. Sci. 41, abstract 1860 (2010).

T. M. Orlando, A. Sprague, G. Greives, D. Schriver, P. Travnicek, J. McLain and R. D. Starr., "Electron-stimulated desorption as a source mechanism for ions in Mercury's space environment", Lunar Planet. Sci. 41, abstract 2246 (2010).

G. A. Grieves, C. A. Hibbitts, M. D. . Dyar, T. M. Orlando, M. Poston and A. Johnson "Mobility and Subsurface Redistribution of Volatiles Through Regolith Materials", Lunar Planet. Sci. 41, abstract 2552 (2010).

G. A. Grieves and T. M. Orlando, "Stimulated reactions on graphite grains and interfaces: A source for CO, CO_2 and HCO", *Ap. J. Lett. Manuscript submitted.*

David Schriver, Pavel Trávníček, Maha Ashour-Abdalla1, Robert L. Richard, Petr Hellinger, James A. Slavin, Brian J. Anderson, Daniel N. Baker, Mehdi Benna, Scott A. Boardsen, Robert E. Gold, George C. Ho, Haje Korth, Stamatios M. Krimigis, William E. McClintock, Thomas M. Orlando, Menelaos Sarantos, Ann L. Sprague, Richard D. Starr, "Electron transport and precipitation at Mercury during the MESSENGER flybys", *Planet. and Space Science*, Manuscript PSS1533 *(see attached abstract)*

Jason L. McLain, Ann L. Sprague, Gregory A. Grieves , David Schriver Pavel Travinicekc and Thomas M. Orlando, "Electron Stimulated Desorption of Silicates: A Potential Source for Ions in Mercury's Space Environment", *J. of Geophys. Research*, Manuscript 2010JE003714 *(see attached abstract).*

Electron Stimulated Desorption of Silicates: A Potential Source for Ions in Mercury's Space Environment

Jason L. McLain[a], Ann L. Sprague[b], Gregory A. Grieves[a], David Schriver[c] Pavel Travinicek[c,d] and Thomas M. Orlando[a]

[a]Georgia Institute of Technology, 901 Atlantic Dr., Atlanta, GA 30332-0400
[b]University of Arizona, Lunar and Planetary Laboratory, 1629 E. University Blvd., Tucson, AZ 85721-0092
[c]Institute of Geophysics and Planetary Physics, UCLA, 3871 Slichter Hall, Los Angeles, CA 90095-1567
[d]Astronomical Institute, ASCR, Prague, Czech Republic, 14131

Corresponding Author:

Thomas M. Orlando
School of Chemistry and Biochemistry and School of Physics
Georgia Institute of Technology
Atlanta, GA 30332-0400
Phone: (404) 894-4012
FAX: (404) 894-7452
thomas.orlando@chemistry.gatech.edu

Abstract

The potential role of electron-stimulated desorption (ESD) in the formation of Mercury's exosphere has been examined. Experimental results involving electron irradiation of Na- and K-bearing silicate glasses yielded direct desorption of H^+, H_2^+, O^+, H_3O^+, Na^+, K^+ and O_2^+. A simulation has also been carried out to calculate electron precipitation fluxes and energies that may be used in the interpretation of measurements made by MESSENGER spacecraft instruments and to better understand the formation of the ion and neutral exosphere at Mercury. The electron fluxes are estimated to be ~10^{10} $cm^{-2}s^{-1}$ with average energies up to 500 eV. The threshold energies for production/release of ions have been measured to be 25±2 eV for H^+, 30±2 eV for O^+, Na^+ and K^+, 40±2 eV for H_2^+ and H_3O^+, and 90±2 eV for O_2^+. The 25-30 eV thresholds correlate with deep valence holes in the O 2s levels that undergo Auger decay. The thresholds for H_2^+ and H_3O^+ correspond to two-hole states in chemisorbed water, which produce energetic protons that undergo reactive scattering on the surface. A significant increase in ESD yield of all ions is observed above a substrate temperature of 350 K. The estimated total cross-section for ESD at a surface temperature of 400 K is ≥10^{-19} cm^2; much larger than neutral production followed by electron impact ionization or photoionization in the gas-phase. These results indicate that ESD may contribute significantly to the production and release of regolith constituents, particularly in ionic form, directly into the exosphere of Mercury.

Keywords: ESD, Auger decay, Mercury, Mercury's exosphere, Magnetospheric interactions

Electron Transport and Precipitation at Mercury During the MESSENGER Flybys

David Schriver[1], Pavel Trávníček [1,3], Maha Ashour-Abdalla[1,2], Robert L. Richard[1], Petr Hellinger[4], James A. Slavin[5], Brian J. Anderson[6], Daniel N. Baker[7], Mehdi Benna[8], Scott A. Boardsen[5], Robert E. Gold[6], George C. Ho[6], Haje Korth[6], Stamatios M. Krimigis[6,9], William E. McClintock[7], Thomas M. Orlando[10], Menelaos Sarantos[6], Ann L. Sprague[11], Richard D. Starr[12]

[1]Institute of Geophysics and Planetary Physics, UCLA, Los Angeles, CA 90095-1567

[2]Department of Physics and Astronomy, UCLA, Los Angeles, CA 90095-1567

[3]Astronomical Institute, ASCR, Prague, Czech Republic, 14131

[4]Department of Space Physics, Institute of Atmospheric Physics, Prague, Czech Republic

[5]Heliophysics Science Division, NASA Goddard Space Flight Center, Greenbelt, MD 20771

[6]Johns Hopkins University Applied Physics Laboratory, Laurel, MD 20723

[7]Laboratory for Atmospheric and Space Physics, University of Colorado, Boulder, CO 80303

[8]Solar System Exploration Division, NASA Goddard Space Flight Center, Greenbelt, MD 20771

[9]Academy of Athens, Office Space Research Technology, Athens 11527, Greece

[10]School of Chemistry and Biochemistry and School of Physics, Georgia Institute of Technology, Atlanta, GA 30332

[11] Lunar and Planetary Laboratory University of Arizona Tucson, AZ 85721

[12]Physics Department, The Catholic University of America, Washington, DC 20064

Abstract

To examine electron transport, energization, and precipitation in Mercury's magnetosphere, a simulation study has been carried out that follows electron trajectories within the global magnetospheric electric and magnetic field configuration of Mercury. We report analysis for two solar-wind parameter conditions corresponding to the first two MESSENGER Mercury flybys on January 14, 2008, and October 6, 2008, which occurred for similar solar wind speed and density, but contrasting interplanetary magnetic field (IMF) directions. During the first flyby the IMF had a northward component, while during the second flyby the IMF was southward. Electron trajectories are traced in the fields of global hybrid simulations for the two flybys. Some solar wind electrons follow complex trajectories at or near where dayside reconnection occurs and enter the magnetosphere at these locations. The entry locations depend on the IMF orientation (north or south). As the electrons move through the entry regions they can be energized as they execute non-adiabatic (demagnetized) motion. Once within the magnetosphere, a fraction of the electrons precipitate at the planetary surface with fluxes the order of 10^9 $cm^{-2}s^{-1}$ and energies of hundreds of eV. This finding may have important implications for the viability of electron-stimulated desorption as a mechanism for contributing to the

formation of the exosphere and heavy ion cloud around Mercury. Some electrons become magnetically trapped and drift around the planet with energies the order of 1-10 keV. The highest energy of electrons anywhere in the magnetosphere is about 25 keV, consistent with the absence of high-energy (> 35 keV) electrons observed during either MESSENGER flyby.